5G Stochastic Channel Model

A Project Report

Submitted by

M.S.AJAY
(EE16B022)

in the partial fulfilment of the requirements
for the award of the degree of

BACHELOR OF TECHNOLOGY
in
ELECTRICAL ENGINEERING

DEPARTMENT OF ELECTRICAL ENGINEERING

INDIAN INSTITUTE OF TECHNOLOGY MADRAS

CHENNAI-600036

JUNE 2020

THESIS CERTIFICATE

This is to certify that the thesis entitled **"5G Stochastic Channel Model"** submitted by **Manchi Sankalkar Ajay** to the Indian Institute of Technology, Madras for the award of the degree of BACHELOR OF TECHNOLOGY in ELECTRICAL ENGINEERING is a bona fide record of research work carried out by him under my supervision. The contents of this thesis, in full or in parts, have not been submitted to any other Institute or University for the award of any degree or diploma.

Prof. Radha Krishna Ganti
Associate Professor
Department of Electrical Engineering
Indian Institute of Technology Madras
Chennai – 600 036.

Table of Contents

List of Figures

Chapter 1
Introduction

1.1. Evolution of cellular standards

The first digital cellular technology, was deployed as 2G in 1990, with voice transmission still being the main use case and an additional option to send text messages and data with speeds of upto 64 kbps over the network. It uses GSM as its key technology and 2G is still the most widespread cellular technology used in India and many other developing countries for voice transmission. There were improvements such as CDMA, GPRS, EDGE done to 2G, which improved the data rates upto 144 kbps and enabled services like email and web-browsing.

3G which used WCDMA as a key technology, came into the picture in 2000 and there was a significant improvement in data speeds, which increased upto 2Mbps when initially deployed and upto 20Mbps later. Global roaming was enabled for the first time and data based applications like video streaming also came into picture with it.

With higher demands for data based applications, the data speeds provided by 3G were not enough and this paved way for 4G in 2010, where even voice was sent over as packets(VOIP) and LTE was the key technology used. It used **OFDM** and **MIMO** as the key

technologies and supports data rates in the range 20-1000 Mbps and thus enabled high quality video streaming and other such applications.

1.2. Motivating factors for deploying 5G

While 4G managed to provide good enough data rates, they were not designed to support extremely high data rates, low latency to support real time applications like automated vehicles or to support a large number of IOT devices, which clearly are the order of the day. These are the key motivating factors to bring in 5G, designed to support upto speeds of 10 Gbps.

1.3. Technologies that provide 5G with significant advantages over 4G

OFDM which is already the main technology used in 4G, has been ramped up in 5G, to optimize the signals sent and pack users in a better way during the implementation of frequency division multiplexing , by the means to support multiple frequency allocation granularities.

The other key technology being Massive MIMO, which includes directional beams targetting specific users, unlike the some of the previous cellular standards where the signals were transmitted all around. This makes energy utilization optimal and enables the ability to serve the users more efficiently. Massive MIMO essentially transmits from several small antenna elements instead of a single antenna that transmit multiple narrow beams, which thus enables beam-forming and also subsequently increases the data capacity that can provided to users in a downlink scenario.

The key factor enabling drastic differences in data speeds in 5G, is the use of mmWave spectrum bands, frequencies above 20GHz. Though there is a flipside of the issue of transmitting signals efficiently at these frequencies, which have been tackled with the help of technologies like phased arrays, they provide much larger bandwidths compared to the lower frequencies used in earlier standards like 700 Mhz or 4GHz, thus increasing the data capacity manifolds.

1.4. Channel Model

The channel model mentioned earlier is built as defined in the ITU document M.2412 defining the evaluation procedures.The document explains in detail about the

small scale and large scale parameters generation procedure for each test environment and usage scenarios, explained in detail in the later part of this report, which are then used to generate the channel coefficients between transmit and recieve antennas.

1.5. My contributions

My project mate Dheeraj contributed in creating the functions required for executing Steps 2 (Prob_LOS), 3(only pathloss excluding indoor loss and in car loss), 5 to 7(delay, power and generation of angles), and Steps 9 – 11. Our work for step-11 included coefficient generation for element to element, later it was developed into antenna array by my fellow project mate Preethi.

My project mate Preethi contributed step-4, 7 and step-11 in upgrading it to the antenna array. She hardcoded all the values from the document to code to generate LSP in step-4. All the means, variances and correlation matrices.

I contributed in step-3 (indoor loss and in car loss), step-8 (coupling) and interpolation of H coefficients using SINC function, calculating field pattern, plotting antenna radiation power pattern and finally SINR distribution.

Chapter 2
Problem Statement

Create the 5G SCM channel model in Matlab to create channel coefficients between individual channels for a set of multiple gNBs and UEs per sector. These coefficients are to be used for getting a received signal when a 5G signal is transmitted. This channel model will be used as a part of the own simulator created in the IITM 5G tested.

Key concepts from Literature Survey

2.1. Introduction to IMT-2020

International Mobile Telecommunications-2020 (IMT-2020) systems are mobile systems that include new radio interface(s) which support the new capabilities of systems beyond IMT-2000 and IMT-Advanced. The ITU-R M.2083 recommendation explains the capabilities of IMT-2020 .

The recommendation aims to make IMT-2020 more flexible, reliable and secure than previous IMT when services are provided in the intended three usage scenarios, namely enhanced mobile broadband (eMBB), ultra-reliable and low-latency communications (URLLC), and massive machine type communications (mMTC).

2.2. Usage Scenarios

The proposed RIT/SRIT shall support a wide range of services across different usage scenarios like:

- ***eMBB*** - Enhanced Mobile Broadband
- ***mMTC*** - Massive machine type communications
- ***URLLC*** - Ultra-reliable and low latency communications

Test environments

A test environment reflects a combination of geographic environment and any one of the usage scenarios listed above. The five environments used for the evaluation procedure are:

- Indoor Hotspot-eMBB
- Dense Urban-eMBB
- Rural-eMBB
- Urban Macro–mMTC
- Urban Macro–URLLC

2.3. Evaluation configurations

Evaluation configurations are defined for the selected test environments. The configuration parameters are applied in analytical and simulation assessments of candidate RITs/SRITs. The technical performance requirement corresponding to that test environment is fulfilled if this requirement is met for one of the evaluation configurations under that specific test environment.

Antenna

2.4. Antenna Characteristics

2.4.1 Base Station Antenna Element Radiation

The field radiation pattern from an antenna element in the azimuthal and zenith directions as a function of the
arrival and departure angles in both directions for transmitter and receiver respectively, to be used for channel coefficients generation are given in the ITU-R M.2412 document.

Figure 1 is antenna 3D radiation pattern of BS antenna element for max gain of 8dBi, frequency of 4GHz. Antenna is along the direction of X axis.

In (Figure 3: elevation cut of Antenna radiation pattern), the 0 angle refers to XY plane.

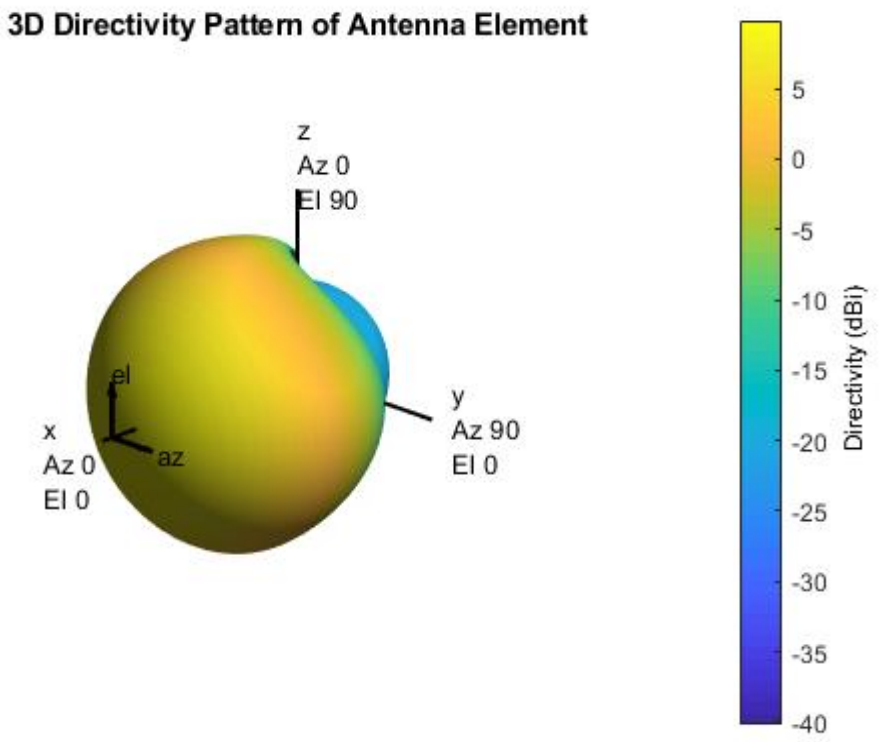

Figure 1: Directional Antenna element 3D radiation pattern, max gain is 8dBi

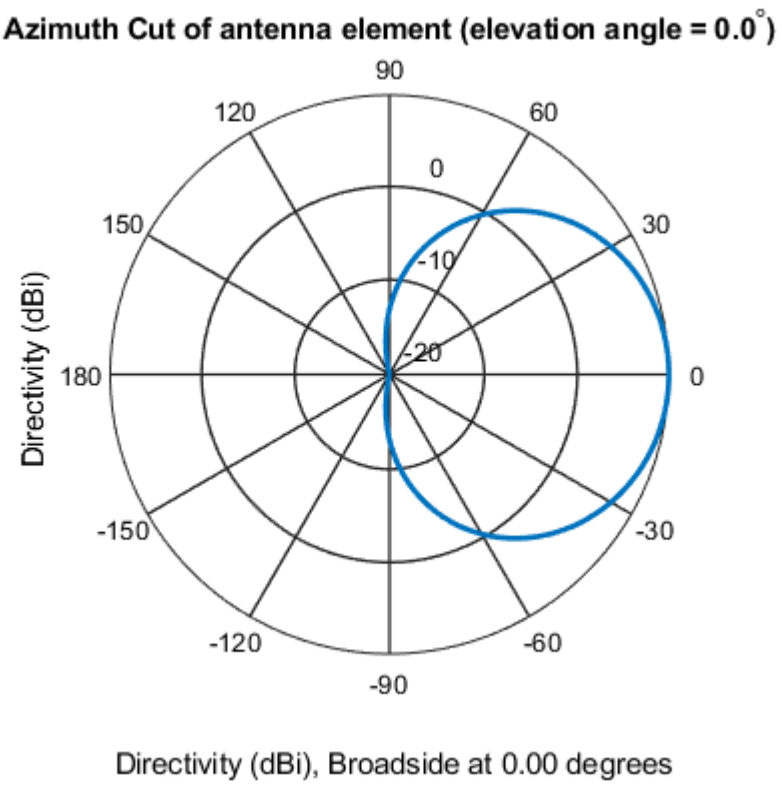

Figure 2 : Azimuthal cut of Antenna radiation pattern

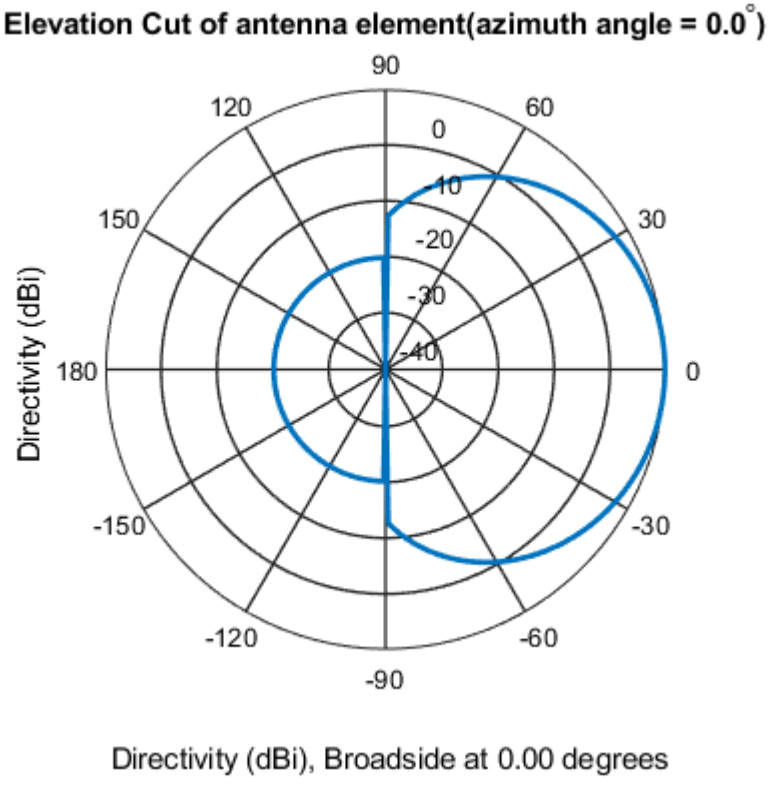

Figure 3: elevation cut of Antenna radiation pattern

2.4.2 UE antenna element radiation

There are two options for UE side antenna element pattern. For 4 GHz and 700 MHz evaluation, Omni-directional antenna element is assumed. For 30GHz and 70GHz directional antenna is considered.

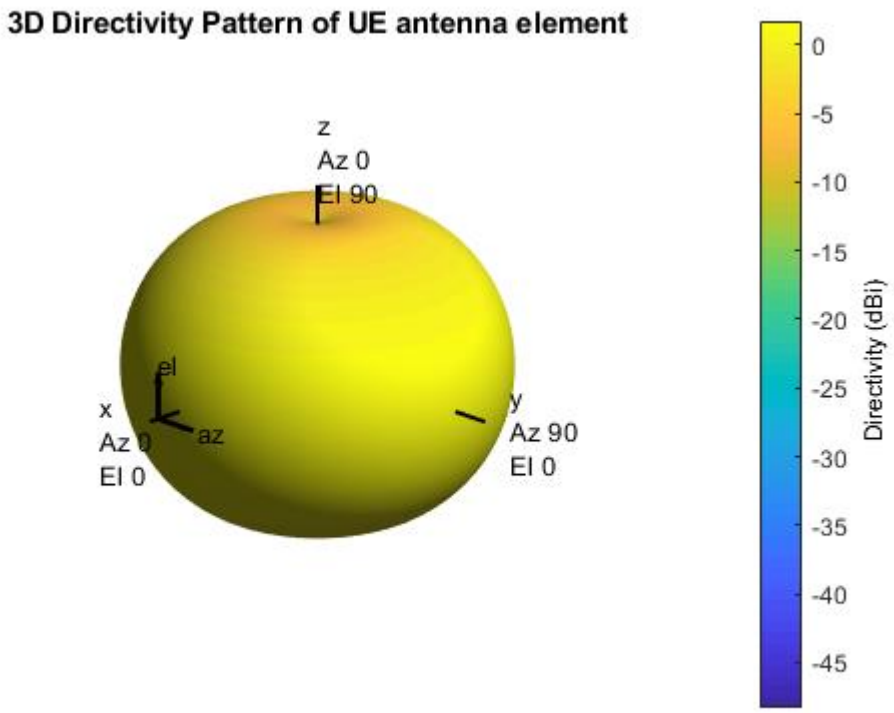

Figure 4: Omni directional Antenna element 3D radiation pattern, max gain is 0dBi

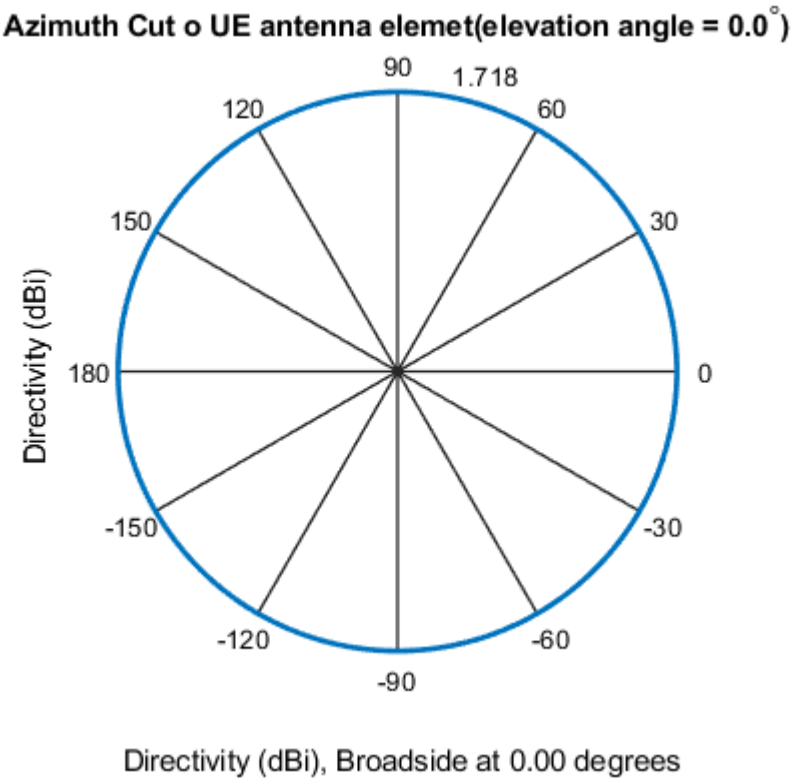

Figure 5: Azimuthal cut of Antenna radiation pattern

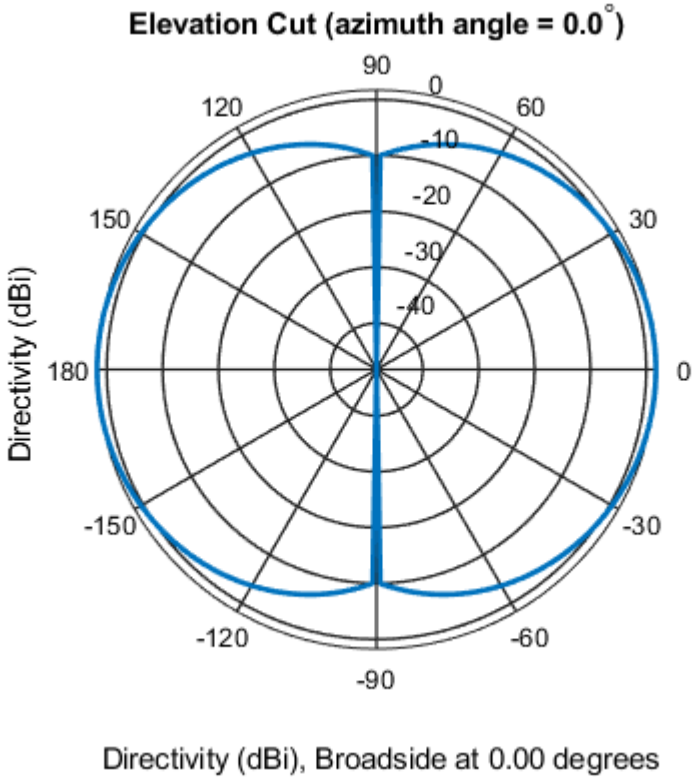

Figure 6: Elevation cut of Antenna radiation

2.4.3 Antenna Array Structure

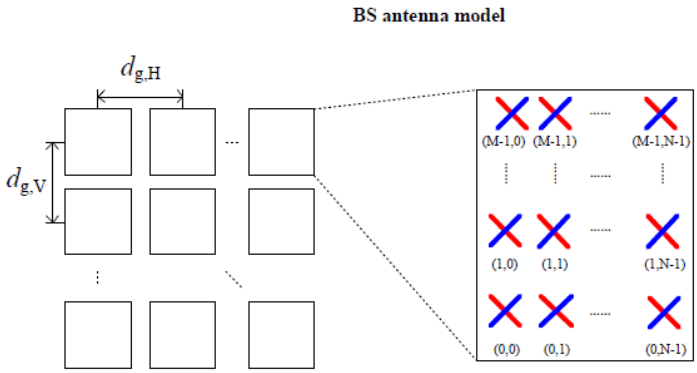

Figure 7: Antenna Array Structure

Antennas are modelled as one or multiple antenna panels, where an antenna panel has one or multiple antenna elements placed in a two-dimensional array within each panel. Each antenna panel has *M*×*N* antenna elements(single or dual polarized), where *N* is the number of columns and *M* is the number of antenna elements with the same polarization in each column. The antenna elements are spaced uniformly with a centre-to-centre distance of d_H horizontally and d_V vertically.

In case of multiple antenna panels, a uniform rectangular panel array is modeled, comprising *MgNg* antenna panels where *Mg* and *Ng* are number of panels in a column and row respectively. Antenna panels are uniformly spaced with a center-to-center spacing of $d_{g,H}$ and $d_{g,V}$ in the horizontal and vertical direction respectively.

The antenna element spacing d_H, d_V, are kept as $\lambda/2$.

Chapter 3
Channel Model Approach

3.1. 5G Stochastic Channel Modelling

Channel modelling is required for realistically modelling the propagation conditions for radio transmission for all required test environments and usage scenarios. There are three IMT-2020 channel modules described in ITU-R M.2412 namely, the primary,

extension and map-based hybrid modules. The project involved modelling the channel based on Primary module, which is a geometry-based stochastic channel model.

A Single Input Single Output (SISO) channel is characterized by two domains, time and frequency and the multipath propagation is defined by attenuation, time delay and path phase.

The Multiple Input Multiple Output (MIMO) channel however is characterized by four domains: Time, Frequency, Space, and Polarization. The channel coefficients depend on transmit and receive antenna characteristics and the propagation characteristics.

The MIMO channel models can either be physical or analytical. Physical models are based on physical theory (often geometrical optics) or on physical measurements. Analytical models are based on mathematical assumptions about the channel behaviour. A physical model further can be either deterministic, where the output of the model is fully determined by the parameter values or stochastic models which possess inherent randomness and the same set of parameter values can lead to an ensemble of output values.

In the Primary Module used for designing the channel model, instead of specifying the location of the scatterers explicitly, the direction of rays are used. This geometry based modelling enables separation of propagation parameters and antennas.

In the absence of environmental scatterers, we get a single pure LOS path.

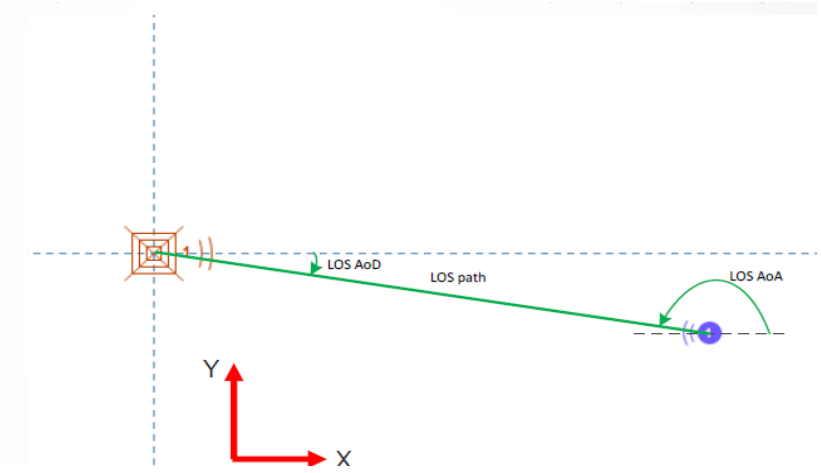

Figure 8: Angles in case of LOS

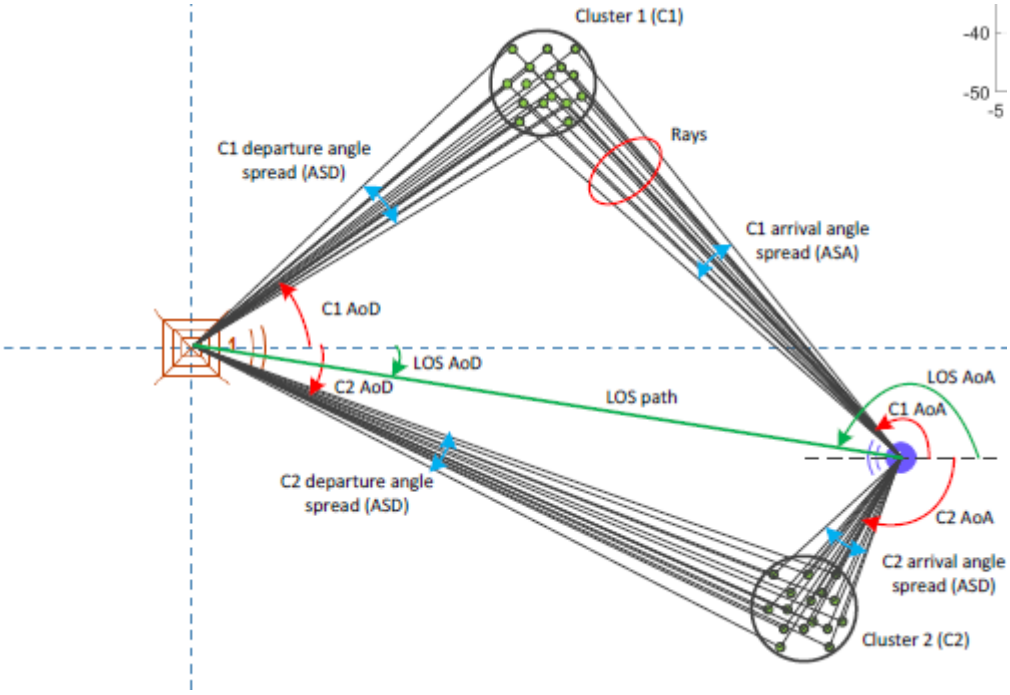

Figure 9: Clusters and their angle spreads

But in the presence of environmental scatterers, multiple propagation paths or (rays) are scattered from buildings etc rather than a LOS path. Scattering from such rough surfaces results as groups of rays close to each dominant propagation path, resulting in the concept of Clusters, as depicted below.

Clusters are defined by angular characteristics like Angular Spread of Departure (ASD), Angular Spread of Arrival (ASA), Angle of Departure (AOD) and Angle of Arrival (AOA) in stochastic models.

The channel parameters are determined stochastically based on statistical distributions from channel measurements. The channel is then realized through the application of the geometrical principle by summing the contributions of rays with specific small-scale parameters like delay, power, azimuth angles of arrival and departure and elevation angles of arrival and departure, which results in correlation of antenna elements and fading due to Doppler as well.

In the absence of a detailed environment database, the precise physical propagation parameters like Direction of Departure (DOD), Direction Of Arrival (DOA), number of paths, path delay, path power are unpredictable, but they have well defined statistical behaviours. Probability models can therefore be constructed for these propagation parameters.

3.2. The 3D MIMO channel model

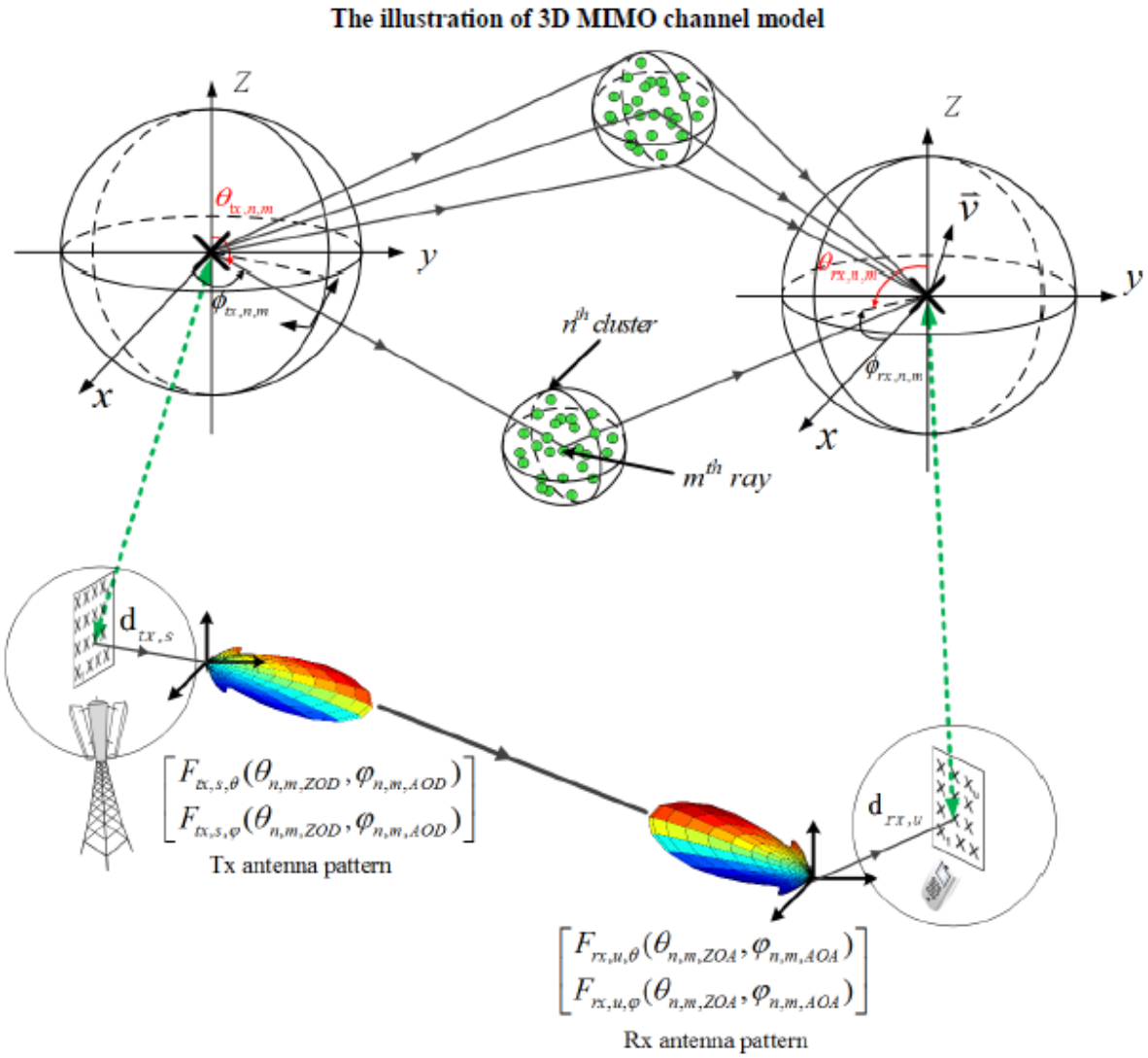

Figure 10: The Illustration of 3D MIMO channel

The above illustration is for a single link channel model. Each circle with several dots represents a scattering region causing one cluster. Each cluster is constituted by *M* rays, and we assume N clusters and *S* antenna elements for transmitter (Tx) and *U* antenna elements for receiver (Rx), respectively. The small-scale parameters like delay $\tau_{n,m}$, azimuth angle of arrival $\varphi_{rx,n,m}$, elevation angle of arrival $\theta_{rx,n,m}$, azimuth angle of departure $\varphi_{tx,n,m}$ and elevation angle of departure $\theta_{tx,n,m}$ are assumed to be different for each ray, where *n , m, u, s* are the indices of the cluster, ray, receiver element and transmitter element respectively. $d_{rx,u}$ and $d_{tx,s}$ are the location vectors of the receive antenna element *u* and transmit antenna element s.

3.3. Test environments in IMT-2020 primary module

IMT-2020 covers the usage scenarios eMBB, URLLC and mMTC across the Indoor Hotspot, Urban and Rural test environments. IMT primary module defines Channel A and B for each of the test environment based on field measurements and are both valid for IMT-2020 candidate evaluations. The mapping of the channel models with the test environments is as shown below.

Test environment	**Indoor Hotspot-eMBB**	**Rural- eMBB**	**Dense Urban - eMBB**	**Urban Macro-URLLC**	**Urban Macro-mMTC**
Channel model	InH_A,InH_B	RMa_A,RMa_B	Macro layer: UMa_A, UMa_B Micro layer: UMi_A, UMi_B	UMa_A,Uma_B	UMa_A,Uma_B

Path loss, Shadow fading and LOS Probability models

The path loss models and their applicability, including frequency ranges and the LOS probability, for the 4 cases of test environments are given in ITU-R M.2412. Shadow fading is modelled as log-normal and the corresponding standard deviation are mentioned along as well.

3.4. Procedure to generate the channel co-efficients

The channel is realised through a detailed step-step procedure consisting of 12 steps as shown below. Apart from this, the advanced channel modelling options described in ITU-R M.2412 can be used for simulating certain cases during the evaluation procedure as well.

The geometric description is such that the arrival angle is from the last scattered bounce and the departure angle is to the first scatterer from the transmitting side. Thus the propagation between the first and last interaction is not defined and this allows for modelling multiple interactions in the scattering media. Therefore parameters like delay can't be deduced from geometry and the procedure for generating such parameters is described in the document.

The following steps are defined for the downlink scenario. For the uplink scenario, the departure and arrival parameters are swapped.

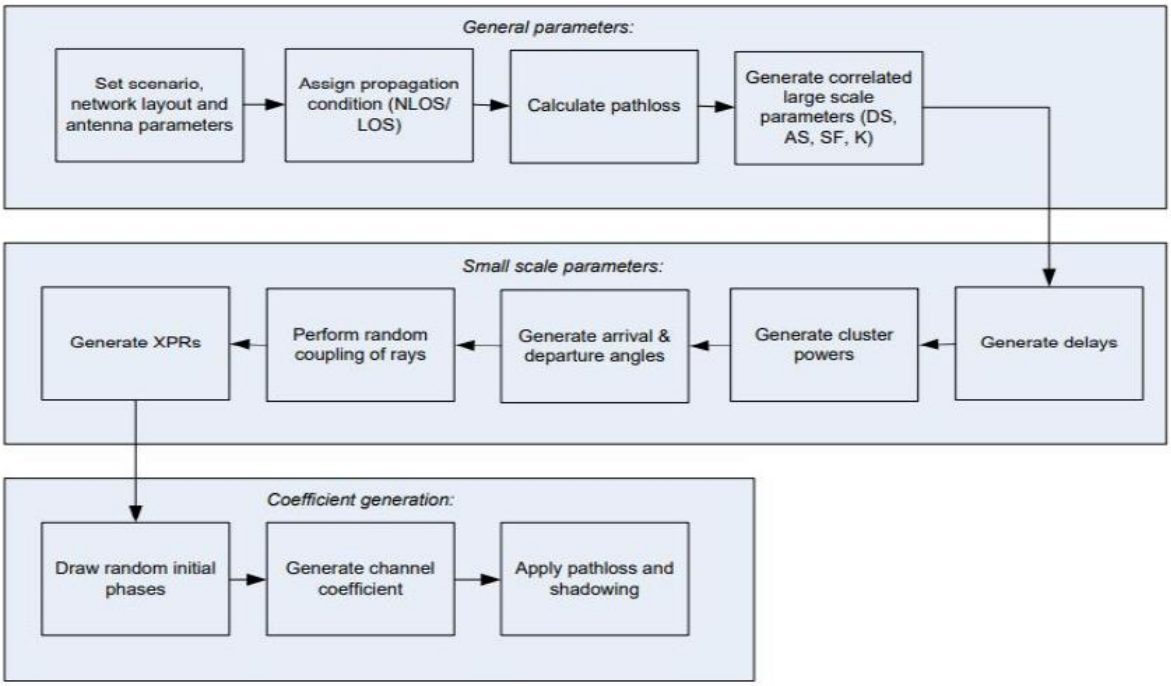

Figure 11:flow chart of channel coefficient generation

3.5. Coordinate System

The coordinate system to be followed is defined by the x,y, z axes, spherical angles and vectors as shown in the figure below. The zenith angle(θ) and azimuth angle(φ) are defined in the Cartesian system as shown below. The spherical basis vectors $\hat{\theta}$ and $\hat{\varphi}$ are defined based on the propogation direction $\hat{n}$. The field component in the direction of $\hat{\theta}$ is given by
F_θ and the field component in the direction of $\hat{\varphi}$ is given by F_φ.

Definition of a global coordinate system showing the zenith angle θ and the azimuth angle ϕ

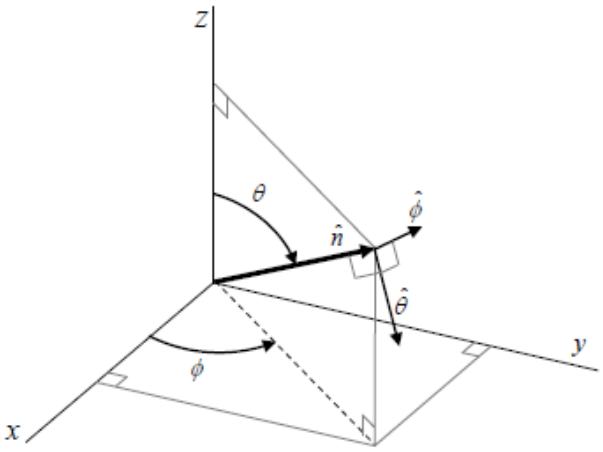

Figure 12: Global coordinate system

3.5.1 Local and global coordinate systems

A Global Coordinate System (GCS) is defined for a system comprising multiple BSs and UTs. An array antenna for a BS or a UT can be defined in a Local Coordinate System (LCS). An LCS is used as a reference to define the vector farfield that is pattern and polarization, of each antenna element in an array. It is assumed that the far-field is known in the LCS by formulae. The placement of an array within the GCS is defined by the translation between the GCS and a LCS.

The orientation of the array with respect to the GCS is defined in general by a sequence of rotations. Since this orientation is in general different from the GCS orientation, it is necessary to map the vector fields of the array elements from the LCS to the GCS. This mapping depends only on the orientation of the array. Arbitrary mechanical orientation of the array can be achieved by rotating the LCS with respect to the GCS. The formulae to map vectors from LCS to GCS is given in [5].

Note that the transformation from a LCS to a GCS depends only on the angles α, β, γ. The angle α is called the bearing angle, β is called the downtilt angle and γ is called the slant angle.

1. $\alpha(bearing\ angle)$: Angle with which LCS is rotated with respect of Z axis of GCS
2. $\beta(downtilt\ angle)$: Angle with which LCS is rotated with respect to Y axis of GCS
3. $\gamma(slant\ angle)$: Angle with which LCS is rotated with respect to X axis of GCS

3.5.2. Example of LCS and GCS

(Figure 1) is antenna radiation pattern in LCS coordinates.

(Figure 13) is antenna radiation in GCS when bearing angle is 120 degrees, and other 2 angles are zero.

(Figure 14) is antenna radiation in GCS when down tilt angle is -45 degrees, and other 2 angles are zero. For ceiling mounted hotspot beta is -90 degrees.

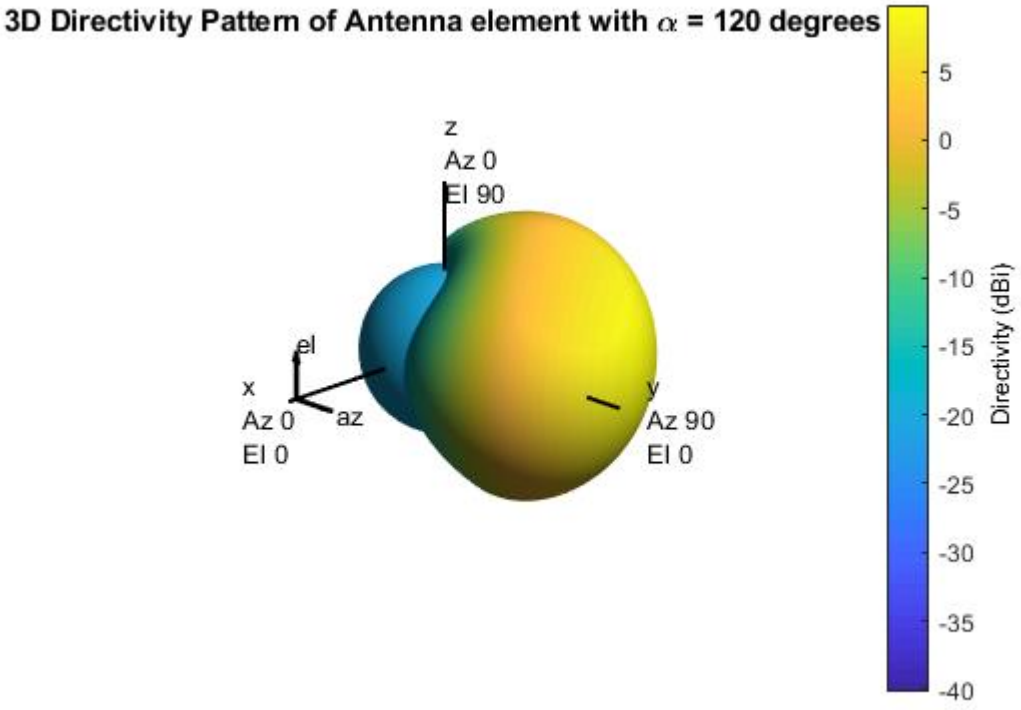

Figure 13: BS antenna element with α(bearing angle) = 120 degrees

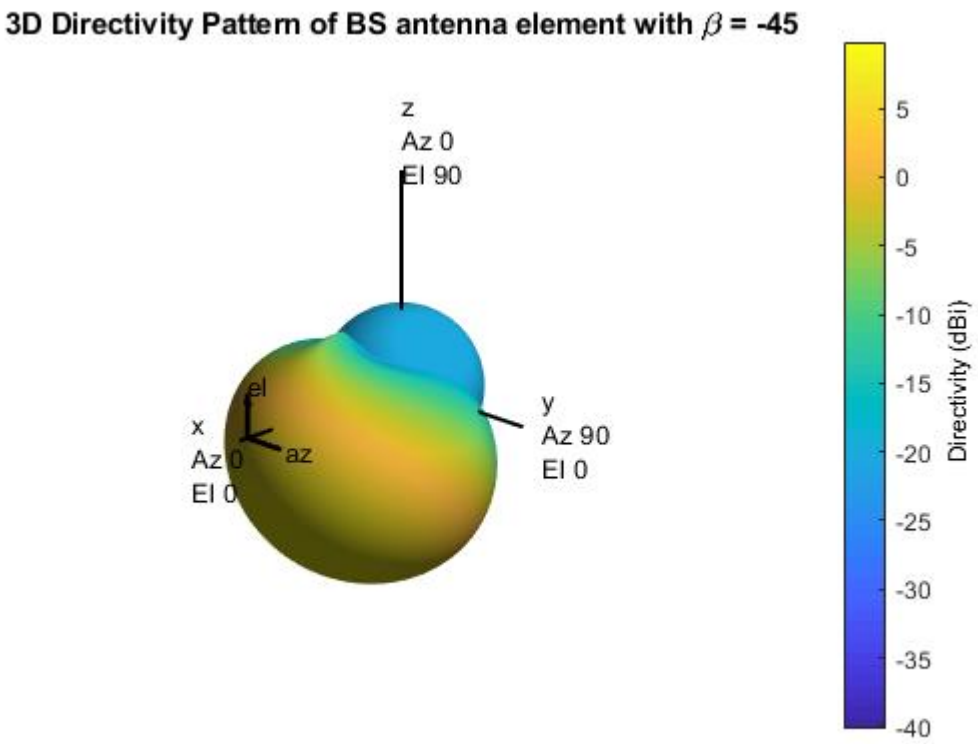

Figure 14: BS antenna element with β(down tilt) =-45 degrees

3.6. Step-by-step procedure

Step 1: Setting environment, network layout, and antenna array parameters

- Choose one of the test environments and corresponding network layouts
- Choose a global coordinate system and define the zenith and azimuth angles and spherical unit vectors as discussed earlier.
- Give the number of Base Station(BS) and User terminals(UT).
- Give 3D location of BS and UT and determine LOS AOD,LOS ZOD,LOS AOA,LOS ZOA.
- Give BS and and UT antenna field patterns F_{rx} and F_{tx} in the global coordinate system and array geometries.
- Give BS and UT array orientations with respect to the global coordinate system
- Array orientation is defined by three angles: Bearing angle,downtilt angle, slant angle
- Give speed and direction of motion of UT in the global coordinate system.
- Give system centre frequency *fc* and bandwidth B.

Generation of large scale parameters (LSPs)

Step 2: Propagation condition LOS/NLOS

- Assign propagation condition (LOS/NLOS).
- The propagation conditions for different BS-UT links are uncorrelated.
- LOS is a probability distribution which depends on distance from BS and height of UT. This distribution is different for indoor and outdoor state.
- Assign an indoor/outdoor state for each UT.
- All the links from a single UT have the same indoor/outdoor state.

Step 3: Modelling and calculation of pathloss

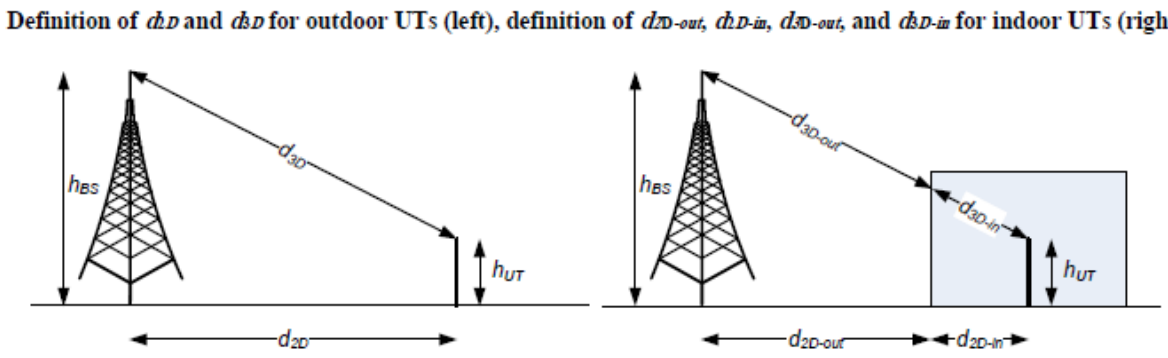

Figure 15: Definition of d2D and d3D

- h_{UT} and h_{BS} are the antenna height at BS and UT, respectively.
- Pathloss depends on LOS/NLOS condition, the distance between BS and UT and frequency of carrier *fc.*
- Different pathloss models has been specified for different test environments in the ITU document for 2 frequency ranges: one in the range 0.5 GHz - 6 GHz and the other, those above 6 GHz.
- In addition to this, outdoor to indoor (O-I) building penetration and car penetration losses should also be taken into account.

Step 4: Generation of other LSPs

Large scale parameters listed below are generated in this step :

- Root-mean-square delay spread (DS)

  The maximum delay time spread is the total time interval during which reflections with significant energy arrive. The r.m.s. delay spread is the standard deviation (or root-mean-square) value of the delay of reflections, weighted proportional to the energy in the reflected waves.

- Root-mean-square angular spreads: Azimuth Angle Spread of Arrival (ASA), Azimuth Angle Spread of Departure (ASD), Zenith Angle Spread of Arrival (ZSA) and Zenith Angle Spread of Departure (ZSD)

- Ricean K-factor (K)

  The ratio of signal power in dominant component over the (local-mean) scattered power.

- Shadow fading (SF)

All these LSPs are correlated and the correlated LSPs are generated taking into account the cross-correlation parameters given in the ITU document using the procedure described in § 3.3.1 of WINNER II Channel Models [4]**.**

Generation of Small scale parameters

Step 5: Generation of delays

Delays are drawn randomly from an exponential delay distribution and are calculated as:

$$\tau_n' = - r_\tau \, DS \, ln \, (X_n)$$

where r_τ is the delay distribution proportionality factor, X_n ~ uniform (0,1), and n is the cluster index n = 1,. . . ,N.

The delays are then normalised by subtracting the minimum delay and are then sorted in the ascending order.

$$\tau_n = sort \, (\tau_n' - min(\tau_n'))$$

In the case of LOS condition, additional scaling of delays is required to compensate for the effect of LOS peak addition to the delay spread. The Ricean K-factor dependent scaling constant is:

$$C_K = 0.7705 - 0.0433 \, K + 0.002 \, K^2 + 0.000017 \, K^3$$

where K [dB] is the Ricean K-factor as generated in Step 4.

The scaled delays $\tau_n^{LOS} = \tau_n / C_K$ are not to be used in cluster power generation.

Step 6: Generation of cluster powers

Cluster powers are calculated, assuming a single slope exponential power delay profile. Power assignment depends on the exponential delay distribution. The cluster

$$P_n' = exp\left(- \tau_n \frac{r_\tau - 1}{r_\tau DS} \right) \cdot 10^{\frac{-Z_n}{10}}$$

powers are determined by:

where $Z_n \sim N(0, \zeta^2)$ is the per cluster shadowing term in [dB]

The cluster powers are then normalised so that the sum power of all cluster powers is equal to one.

$$P_n = \frac{P_n^{'}}{\sum_{n=1}^{N} P_n^{'}}$$

In the case of LOS condition, an additional specular component is added to the first cluster. The power of the single LOS ray is given by:

$$P_{1,LOS} = \frac{K_R}{K_R + 1}$$

And the cluster powers are given by:

$$P_n = \frac{1}{K_R + 1} \frac{P_n'}{\sum_{n=1}^{N} P_n'} + \delta(n-1) P_{1,LOS}$$

The power of each ray within a cluster is assigned as *Pn/M*, where *M* is the number of rays per cluster. The clusters with less than –25 dB power compared to the maximum cluster power are then removed.

Step 7: Generation of arrival and departure angles in both dimensions

Angle generation in azimuth direction

The composite Power Azimuth Spectrum(PAS) in azimuth of all clusters can be modelled as wrapped Gaussian or Laplacian. The AOAs are determined by applying the inverse Gaussian function equation or the inverse Laplacian function equation with input parameters P_n and RMS angle spread ASA, respectively.

$$\text{Gaussian: } \varphi_{n,AOA}' = \frac{2(\text{ASA}/1.4)\sqrt{-\ln\left(P_n/\max\left(P_n\right)\right)}}{C_\varphi}$$

$$\text{Laplacian: } \phi_{n,AOA}' = -\frac{\text{ASA}\ln\left(P_n/\max\left(P_n\right)\right)}{C_\phi}$$

with C_ϕ defined as:

$$\text{Guassian: } C_\phi = \begin{cases} C_\phi^{\text{NLOS}} \cdot \left(1.1035 - 0.028K - 0.002K^2 + 0.0001K^3\right) & \text{,for LOS} \\ C_\phi^{\text{NLOS}} & \text{,for NLOS} \end{cases},$$

$$\text{Laplacian: } C_\phi = \begin{cases} C_\phi^{\text{NLOS}} \cdot \left(0.9275 + 0.0439K - 0.0071K^2 + 0.0002K^3\right) & \text{,for LOS} \\ C_\phi^{\text{NLOS}} & \text{,for NLOS} \end{cases},$$

where C_φ^{NLOS} is defined as a scaling factor related to the total number of clusters and the values for each cluster for both Laplacian and Gaussian distributions are given in the document.

A positive or negative sign is assigned to the angles by multiplying with a random variable X_n with uniform distribution to the discrete set of {1,–1}, and add a component Y_n ~ N (0, (ASA/7)^2) to introduce a random variation.

$$\phi_{n,AOA} = X_n\phi'_{n,AOA} + Y_n + \phi_{LOS,AOA}$$

where $\varphi_{LOS,AOA}$ is the LOS direction defined in the network layout description as mentioned in Step 1.

In the LOS case, the constant C_φ also depends on the Ricean K-factor in [dB], as generated in Step 4. Additional scaling of the angles is required to compensate for the effect of LOS peak addition to the angle spread.

In the LOS case, instead of the above equation, the below equation is used so that the first cluster is forced to the LOS direction $\varphi_{LOS,\,AOA}$:

$$\phi_{n,AOA} = \left(X_n\phi'_{n,AOA} + Y_n\right) - \left(X_1\phi'_{1,AOA} + Y_1 - \phi_{LOS,AOA}\right)$$

Ray offset angles α_m for each of the rays within a cluster, are given for rms angle spread normalized to 1, in the document. These are added to the cluster angles as shown below:

$$\phi_{n,m,AOA} = \phi_{n,AOA} + c_{ASA}\alpha_m$$

where c_{ASA} is the cluster-wise rms azimuth spread of arrival angles (cluster ASA), which are also given in the document. The generation of AOD ($\varphi_{n,m,AOD}$) follows a procedure similar to AOA as described above.

Angle generation in zenith direction

The composite Power Azimuth Spectrum(PAS) in zenith of all clusters are modelled as Laplacian. The ZOAs are determined by applying the inverse Laplacian function equation with input parameters P_n and RMS angle spread ZSA, respectively.

$$\theta'_{n,ZOA} = -\frac{\mathrm{ZSA}\, ln(P_n / max(P_n))}{C_\theta}$$

For channel model A, C_θ is defined as:

$$C_\theta = \begin{cases} C_\theta^{\mathrm{NLOS}} \cdot \left(1.35 + 0.0202K - 0.0077K^2 + 0.0002K^3\right) & \text{, for LOS} \\ C_\theta^{\mathrm{NLOS}} & \text{, for NLOS} \end{cases}$$

For channel model B, C_θ is defined as:

$$C_\theta = \begin{cases} C_\theta^{\mathrm{NLOS}} \cdot \left(1.3086 + 0.0339K - 0.0077K^2 + 0.0002K^3\right) & \text{, for LOS} \\ C_\theta^{\mathrm{NLOS}} & \text{, for NLOS} \end{cases}$$

Where C_θ^{NLOS} is defined as a scaling factor related to the total number of clusters and the values for each cluster for the Laplacian distribution are given in the document.

A positive or negative sign is assigned to the angles by multiplying with a random variable X_n with uniform distribution to the discrete set of {1,–1}, and add a component Y_n ~ N (0, (ASA/7)^2) to introduce a random variation.

$$\theta_{n,ZOA} = X_n \theta'_{n,ZOA} + Y_n + \bar{\theta}_{ZOA},$$

where $\bar{\theta}_{ZOA}$ = 90° if the BS-UT link is O2I and $\bar{\theta}_{ZOA} = \theta_{LOS,ZOA}$ which is the LOS direction defined in the network layout description as mentioned in Step 1.

In the LOS case, instead of the above equation, the below equation is used so that the first cluster is forced to the LOS direction $\theta_{LOS,ZOA}$:

$$\theta_{n,ZOA} = \left(X_n \theta'_{n,ZOA} + Y_n\right) - \left(X_1 \theta'_{1,ZOA} + Y_1 - \theta_{LOS,ZOA}\right).$$

Ray offset angles α_m for each of the rays within a cluster, are given for rms angle spread normalized to 1, in the document. These are added to the cluster angles as shown below:

$$\theta_{n,m,ZOA} = \theta_{n,ZOA} + c_{ZSA}\alpha_m$$

where c_{zSA} is the cluster-wise rms azimuth spread of arrival angles (cluster ZSA), which are also given in the document.

The generation of ZOD ($\theta_{n,m,ZOD}$) follows a similar procedure.

$$\theta_{n,ZOD} = X_n\theta'_{n,ZOD} + Y_n + \theta_{LOS,ZOD} + \mu_{offset,ZOD}$$

where X_n is a variable with uniform distribution to the discrete set of {1,–1},
Y_n ~ N (0, (ASA/7)^2) and the values for $\mu_{offset,ZOD}$ are mentioned in the document.

Ray offset angles α_m for each of the rays within a cluster, are given for rms angle spread normalized to 1, in the document. These are added to the cluster angles as shown below:

$$\theta_{n,m,ZOD} = \theta_{n,ZOD} + (3/8)(10^{\mu_{1gZSD}})\alpha_m$$

where μ_{1gZSD} is the mean of the ZSD log-normal distribution.

In the LOS case, the generation of ZOD follows the same procedure as ZOA described above using equation.

Step 8: Coupling of rays within a cluster for both dimensions

- Couple randomly AOD angles $\varphi_{n,m,AOD}$ to AOA angles $\varphi_{n,m,AOA}$ within a cluster n, or within a subcluster in the case of two strongest clusters (described in Step 11).
- Couple randomly ZOD angles $\theta_{n,m,ZOD}$ with ZOA angles $\theta_{n,m,ZOA}$ using the same procedure.
- Also, Couple randomly AOD angles $\varphi_{n,m,AOD}$ with ZOD angles $\theta_{n,m,ZOD}$ using the same procedure.

Step 9: Generation of cross polarization power ratios

The cross polarization power ratios *K* (XPR) are generated for each ray ***m*** of each cluster ***n***. XPR is log-normal distributed. The XPR values are drawn as shown below:

$$K_{n,m} = 10^{X/10}$$

where $X \sim N(\mu_{XPR}, \sigma^2_{XPR})$ is Gaussian distributed with μ_{XPR}, σ^2_{XPR} values given in the document.

Generation of channel coefficients

Step 10: Drawing of initial phases

The initial phase $\{ \Phi_{n,m}^{\theta\theta}, \Phi_{n,m}^{\theta\varphi}, \Phi_{n,m}^{\varphi\theta}, \Phi_{n,m}^{\varphi\varphi} \}$ is drawn randomly for each ray *m* of each cluster *n* and for four different polarisation combinations (θθ, θφ, φθ and φφ). The distribution for initial phases is uniform within (-π, +π). It is added to ensure a random starting point for fast fading.

In the LOS case, if Φ_{LOS} is chosen as a random variable, then a random initial phase for both θθ and φφ polarisations are drawn.

Step 11: Generation of channel coefficients

Channel impulse response generation for a single link(Single antenna panel at both tx and rx)

The channel coefficients are generated for each cluster *n* and each receiver and transmitter element pair *u, s*.

For the *N – 2* weakest clusters, say n = 3, 4,…, *N*, the channel coefficients are given by:

$$H_{u,s,n}^{\mathrm{NLOS}}(t) = \sqrt{\frac{P_n}{M}} \sum_{m=1}^{M} \begin{bmatrix} F_{rx,u,\theta}\left(\theta_{n,m,ZOA}, \varphi_{n,m,AOA}\right) \\ F_{rx,u,\varphi}\left(\theta_{n,m,ZOA}, \varphi_{n,m,AOA}\right) \end{bmatrix}^{T} \begin{bmatrix} \exp\left(j\Phi_{n,m}^{\theta\theta}\right) & \sqrt{\kappa_{n,m}^{-1}} \exp\left(j\Phi_{n,m}^{\theta\varphi}\right) \\ \sqrt{\kappa_{n,m}^{-1}} \exp\left(j\Phi_{n,m}^{\varphi\theta}\right) & \exp\left(j\Phi_{n,m}^{\varphi\varphi}\right) \end{bmatrix}$$
$$\begin{bmatrix} F_{tx,s,\theta}\left(\theta_{n,m,ZOD}, \varphi_{n,m,AOD}\right) \\ F_{tx,s,\varphi}\left(\theta_{n,m,ZOD}, \varphi_{n,m,AOD}\right) \end{bmatrix} \exp\left(j2\pi \frac{\hat{r}_{rx,n,m}^{T} . \overline{d}_{rx,u}}{\lambda_0} \right) \exp\left(j2\pi \frac{\hat{r}_{tx,n,m}^{T} . \overline{d}_{tx,s}}{\lambda_0} \right) \exp\left(j2\pi \frac{\hat{r}_{rx,n,m}^{T} . \overline{v}}{\lambda_0} t \right)$$

where $F_{rx,u,\theta}$ and $F_{rx,u,\varphi}$ are the field patterns of receive antenna element *u* in the direction of the spherical basis vectors, $\hat{\theta}$ and $\hat{\varphi}$ respectively, $F_{tx,s,\theta}$ and $F_{tx,s,\varphi}$ are the field patterns of transmit antenna element *s* in the direction of the spherical basis vectors, $\hat{\theta}$ and $\hat{\varphi}$ respectively.

$\hat{r}_{rx,n,m}$ is the spherical unit vector with azimuth arrival angle $\varphi_{n,m,AOA}$ and elevation arrival angle $\theta_{n,m,ZOA}$, given by:

$$\hat{r}_{rx,n,m} = \begin{bmatrix} \sin\theta_{n,m,ZOA} \cos\varphi_{n,m,AOA} \\ \sin\theta_{n,m,ZOA} \sin\varphi_{n,m,AOA} \\ \cos\theta_{n,m,ZOA} \end{bmatrix}$$

where *n* denotes a cluster and *m* denotes a ray within cluster *n*.

$\hat{r}_{tx,n,m}$ is the spherical unit vector with azimuth departure angle $\varphi_{n,m,AOD}$ and elevation departure angle $\theta_{n,m,ZOD}$, given by:

$$\hat{r}_{tx,n,m} = \begin{bmatrix} \sin\theta_{n,m,ZOD}\cos\varphi_{n,m,AOD} \\ \sin\theta_{n,m,ZOD}\sin\varphi_{n,m,AOD} \\ \cos\theta_{n,m,ZOD} \end{bmatrix}$$

where *n* denotes a cluster and *m* denotes a ray within cluster *n*.

$\bar{d}_{rx,u}$ is the location vector of receive antenna element *u* and $\bar{d}_{tx,s}$ is the location vector of transmit antenna element s, $K_{n,m}$ is the cross polarisation power ratio in linear scale, and λ_0 is the wavelength of the carrier frequency. If polarisation is not considered, the 2×2 polarisation matrix can be replaced by the scalar $exp(j\Phi_{n,m})$ and only vertically polarised field patterns are applied.

The Doppler frequency component depends on the arrival angles (AOA, ZOA), and the UT velocity vector $\bar{\boldsymbol{v}}$ with speed *v*, travel azimuth angle φ_v, elevation angle θ_v and is given by:

$$v_{n,m} = \frac{\hat{r}_{rx,n,m}^{T}\cdot\bar{v}}{\lambda_0}, \text{where } \bar{v} = v.\begin{bmatrix} sin\,\theta_v\,cos\,\phi_v & sin\,\theta_v\,sin\,\phi_v & cos\,\theta_v \end{bmatrix}^T$$

For the two strongest clusters, say n = 1 and 2, rays are spread in delay to three sub-clusters (per cluster), with a fixed delay offset.

The delays of the sub-clusters are

$$\tau_{n,1} = \tau_n$$
$$\tau_{n,2} = \tau_n + 1.28\ c_{DS}$$
$$\tau_{n,3} = \tau_n + 2.56\ c_{DS}$$

where c_{DS} is the cluster delay spread, the values for which are given in the document.

The twenty rays within these two clusters are mapped to three sub clusters as shown below:

Sub-cluster information for intra cluster delay spread clusters

sub-cluster # i	**mapping to rays** $\mathcal{R}_i$	**Power** $\lvert\mathcal{R}_i\rvert/M$	**delay offset** $\tau_{n,i} - \tau_n$
$i = 1$	$\mathcal{R}_1 = \{1,2,3,4,5,6,7,8,19,20\}$	10/20	0
$i = 2$	$\mathcal{R}_2 = \{9,10,11,12,17,18\}$	6/20	$1.28\ c_{DS}$
$i = 3$	$\mathcal{R}_3 = \{13,14,15,16\}$	4/20	$2.56\ c_{DS}$

The channel impulse response is then given by:

$$H_{u,s}^{\mathrm{NLOS}}(\tau,t)=\sum_{n=1}^{2}\sum_{i=1}^{3}\sum_{m\in R_i}H_{u,s,n,m}^{\mathrm{NLOS}}(t)\delta(\tau-\tau_{n,i})+\sum_{n=3}^{N}H_{u,s,n}^{\mathrm{NLOS}}(t)\delta(\tau-\tau_n)$$

where $H_{u,s,n,m}^{\mathrm{NLOS}}(t)$ is defined as:

$$H_{u,s,n,m}^{\mathrm{NLOS}}(t)=\sqrt{\frac{P_n}{M}}\begin{bmatrix}F_{rx,u,\theta}\left(\theta_{n,m,ZOA},\varphi_{n,m,AOA}\right)\\F_{rx,u,\varphi}\left(\theta_{n,m,ZOA},\varphi_{n,m,AOA}\right)\end{bmatrix}^{T}\begin{bmatrix}\exp\left(j\Phi_{n,m}^{\theta\theta}\right) & \sqrt{\kappa_{n,m}^{-1}}\exp\left(j\Phi_{n,m}^{\theta\varphi}\right)\\\sqrt{\kappa_{n,m}^{-1}}\exp\left(j\Phi_{n,m}^{\varphi\theta}\right) & \exp\left(j\Phi_{n,m}^{\varphi\varphi}\right)\end{bmatrix}$$
$$\begin{bmatrix}F_{tx,s,\theta}\left(\theta_{n,m,ZOD},\varphi_{n,m,AOD}\right)\\F_{tx,s,\varphi}\left(\theta_{n,m,ZOD},\varphi_{n,m,AOD}\right)\end{bmatrix}\exp\left(j2\pi\frac{\hat{r}_{rx,n,m}^{T}.\bar{d}_{rx,u}}{\lambda_0}\right)\exp\left(j2\pi\frac{\hat{r}_{tx,n,m}^{T}.\bar{d}_{tx,s}}{\lambda_0}\right)\exp\left(j2\pi\frac{\hat{r}_{rx,n,m}^{T}.\bar{v}}{\lambda_0}t\right)$$

In the above equations, δ(.) is the Dirac delta function.

The channel response is generated by adding the LOS channel coefficient to the NLOS channel impulse response and scaling the two terms by the desired Ricean K factor K_R.

$$H_{u,s}^{\mathrm{LOS}}(\tau,t)=\sqrt{\frac{1}{K_R+1}}H_{u,s}^{\mathrm{NLOS}}(\tau,t)+\sqrt{\frac{K_R}{K_R+1}}H_{u,s,1}^{\mathrm{LOS}}(t)\delta(\tau-\tau_1)$$

3.7. Channel impulse response generation for antenna arrays

In this model there are Multiple antenna panels at both tx and rx.

Arrangement of the antenna arrays

The antenna panel which is arranged in a uniform rectangular array and the cross-polarised elements within them are arranged as shown below.

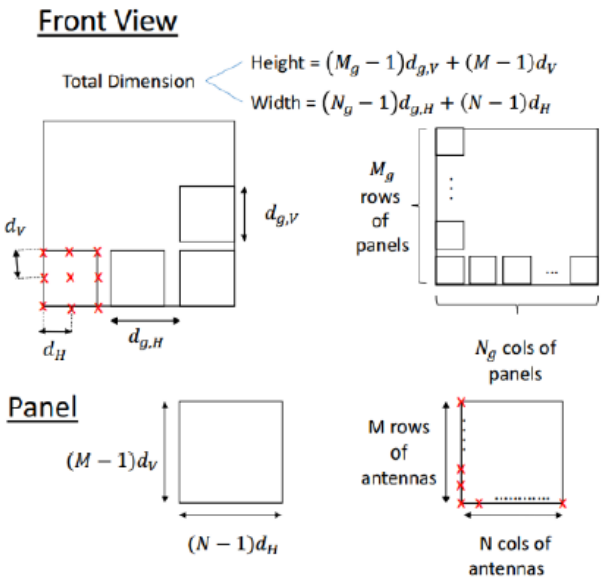

where ,

- *Mg* and *Ng* are number of panels in a column and row respectively.
- Antenna panels are uniformly spaced with a center-to-center spacing of $d_{g,H}$ and $d_{g,V}$ in the horizontal and vertical direction respectively.
- Each antenna panel has *M*×*N* antenna elements (single or dual polarized), where *N* is the number of columns and *M* is the number of antenna elements with the same polarization in each column.
- The antenna elements are spaced uniformly with a centre-to-centre distance of d_H horizontally and d_V vertically.

In case of a single cross polarized antenna, *Mg = Ng = M = N =1* . In case of a uniform rectangular array of cross polarized antennas with no sub arrays *Mg = Ng = 1.*

Vector channel response

Using antenna arrays at the transmitter and receiver results in a vector channel response. The LOS channel coefficient and NLOS channel impulse response for each cluster *n* is given below:

$$\mathbf{H}_n^{\mathrm{NLOS}}(t)=\sqrt{\frac{P_n}{M}}\sum_{m=1}^{M}\begin{bmatrix}F_{\mathrm{rx},\theta}\left(\theta_{n,m,ZOA},\phi_{n,m,AOA}\right)\\F_{\mathrm{rx},\phi}\left(\theta_{n,m,ZOA},\phi_{n,m,AOA}\right)\end{bmatrix}^{T}\begin{bmatrix}\exp\left(j\Phi_{n,m}^{\theta\theta}\right) & \sqrt{\kappa_{n,m}^{-1}}\exp\left(j\Phi_{n,m}^{\theta\phi}\right)\\\sqrt{\kappa_{n,m}^{-1}}\exp\left(j\Phi_{n,m}^{\phi\theta}\right) & \exp\left(j\Phi_{n,m}^{\phi\phi}\right)\end{bmatrix}$$
$$\times\begin{bmatrix}F_{\mathrm{tx},\theta}\left(\theta_{n,m,ZOD},\phi_{n,m,AOD}\right)\\F_{\mathrm{tx},\phi}\left(\theta_{n,m,ZOD},\phi_{n,m,AOD}\right)\end{bmatrix}\mathbf{a}_{\mathrm{rx}}\left(\theta_{n,m,ZOA},\phi_{n,m,AOA}\right)\mathbf{a}_{\mathrm{tx}}^{\mathrm{H}}\left(\theta_{n,m,ZOD},\phi_{n,m,AOD}\right)\exp\left(j2\pi v_{n,m}t\right)$$

$$\mathbf{H}_n^{\mathrm{LOS}}(t)=\begin{bmatrix}F_{\mathrm{rx},\theta}\left(\theta_{LOS,ZOA},\phi_{LOS,AOA}\right)\\F_{\mathrm{rx},\phi}\left(\theta_{LOS,ZOA},\phi_{LOS,AOA}\right)\end{bmatrix}^{T}\begin{bmatrix}\exp\left(j\Phi_{LOS}\right) & 0\\0 & \exp\left(j\Phi_{LOS}\right)\end{bmatrix}$$
$$\times\begin{bmatrix}F_{\mathrm{tx},\theta}\left(\theta_{LOS,ZOD},\phi_{LOS,AOD}\right)\\F_{\mathrm{tx},\phi}\left(\theta_{LOS,ZOD},\phi_{LOS,AOD}\right)\end{bmatrix}\mathbf{a}_{\mathrm{rx}}\left(\theta_{LOS,ZOA},\phi_{LOS,AOA}\right)\mathbf{a}_{\mathrm{tx}}^{\mathrm{H}}\left(\theta_{LOS,ZOD},\phi_{LOS,AOD}\right)\exp\left(j2\pi v_{\mathrm{LOS}}t\right)$$

where $\mathbf{a}_{rx}(\theta_{n,m,ZOA}, \varphi_{n,m,AOA})$ and $\mathbf{a}_{tx}(\theta_{n,m,ZOD}, \varphi_{n,m,AOD})$ are the rx and tx antenna array response vectors respectively, of rays $m \in 1,2,\ldots,M$ in the cluster $n \in 1,2,\ldots,N$. They are given by:

$$\mathbf{a}_{\mathrm{tx}}\left(\theta_{n,m,ZOD},\phi_{n,m,AOD}\right)=\exp(j\frac{2\pi}{\lambda}(\mathbf{W}_{tx}\mathbf{r}_{\mathrm{tx}}(\theta_{n,m,ZOD},\phi_{n,m,AOD}))),\forall n,m,$$

$$\mathbf{a}_{\mathrm{rx}}\left(\theta_{n,m,ZOA},\phi_{n,m,AOA}\right)=\exp(j\frac{2\pi}{\lambda}(\mathbf{W}_{\mathrm{rx}}\mathbf{r}_{\mathrm{rx}}(\theta_{n,m,ZOA},\phi_{n,m,AOA}))),\forall n,m,$$

where λ is the wavelength of the carrier frequency f, $\mathbf{r}_{rx}(\theta_{n,m,ZOA}, \varphi_{n,m,AOA})$ and $\mathbf{r}_{tx}(\theta_{n,m,ZOD}, \varphi_{n,m,AOD})$ are the corresponding angular 3 x 1 spherical unit vectors of the rx and tx, respectively.

$\mathbf{W}_{tx}$ and $\mathbf{W}_{rx}$ are the location matrices of the tx and rx antenna elements in 3D Cartesian coordinates, which are provided for an uniform rectangular array antenna configuration consisting of cross polarized antenna elements and for the arrangement discussed above earlier. For the uniform rectangular array configuration discussed above, $\mathbf{W}_{tx}$ and $\mathbf{W}_{rx}$ are matrices of the dimension $2NMN_gM_g$ x 3.

$\mathbf{W}_{tx}$ for example, = [w_{ij}] i=1,2, . . , $2NMN_gM_g$, j =1,2,3, where

$$w_{ij}=\begin{cases}0, & j=1\\\left\lfloor\left(i-1-2N\left\lfloor\frac{i-1}{2N}\right\rfloor\right)/2\right\rfloor\cdot d_H+\left\lfloor\left(i-1-2NN_g\left\lfloor\frac{i-1}{2NN_g}\right\rfloor\right)/(2N)\right\rfloor\cdot d_{g,H}, & j=2\\\left\lfloor\left(i-1-2NMN_g\left\lfloor\frac{i-1}{2NMN_g}\right\rfloor\right)/(2NN_g)\right\rfloor\cdot d_V+\left\lfloor\left(i-1-2NMN_gM_g\left\lfloor\frac{i-1}{2NMN_gM_g}\right\rfloor\right)/(2NMN_g)\right\rfloor\cdot d_{g,V}, & j=3\end{cases}$$

The spherical unit vectors are given by:

$$\mathbf{r}_{\mathrm{rx},n,m} = \begin{bmatrix} \sin\theta_{n,m,ZOA}\cos\varphi_{n,m,AOA} \\ \sin\theta_{n,m,ZOA}\sin\varphi_{n,m,AOA} \\ \cos\theta_{n,m,ZOA} \end{bmatrix}$$

$$\mathbf{r}_{\mathrm{tx},n,m} = \begin{bmatrix} \sin\theta_{n,m,ZOD}\cos\varphi_{n,m,AOD} \\ \sin\theta_{n,m,ZOD}\sin\varphi_{n,m,AOD} \\ \cos\theta_{n,m,ZOD} \end{bmatrix}$$

The Doppler frequency component $v_{n,m}$ depends on the arrival angles (AOA, ZOA), and the UT velocity vector $\bar{\boldsymbol{v}}$ with speed v, travel azimuth angle φ_v, elevation angle θ_v and is given by:

$$v_{n,m} = \frac{\mathbf{r}_{rx,n,m}^{T}.\bar{v}}{\lambda_0}$$

$$\bar{v} = v.\left[\sin\theta_v\cos\varphi_v \quad \sin\theta_v\sin\varphi_v \quad \cos\theta_v\right]^T$$

Step 12: Path loss and shadowing

Apply path loss and shadowing for the channel coefficients.

Chapter 4
Results and Discussions

4.1. SINR

For generating SINR, we have taken 7 gnB s arranged in hexagon pattern. Each gnB has 3 sectors. Each gNB has three antenna directed along each sector. These three antenna has bearing angles 0,120,240 degrees. The hexagon grid for Urban profile is shown in Figure 16 with inter site distance 200m. In Figure 16 the red dots are Base stations.

We have taken a meshgrid of points. For each point, Received power from each antenna (P_i) is calculated. The antenna from which received power is maximum, that antenna is considered and all other signal from other antennas are considered as interference.

Noise = $10^{0.1*(-174dBm+10*log10(BW)+noise\ figure)}$

SINR at a point = $\max(P_i)\ /(\Sigma P_i - \max(\mathrm{P_i}) + \mathrm{Noise})$.

Where P_i= received power from i^{th} antenna to the point in meshgrid

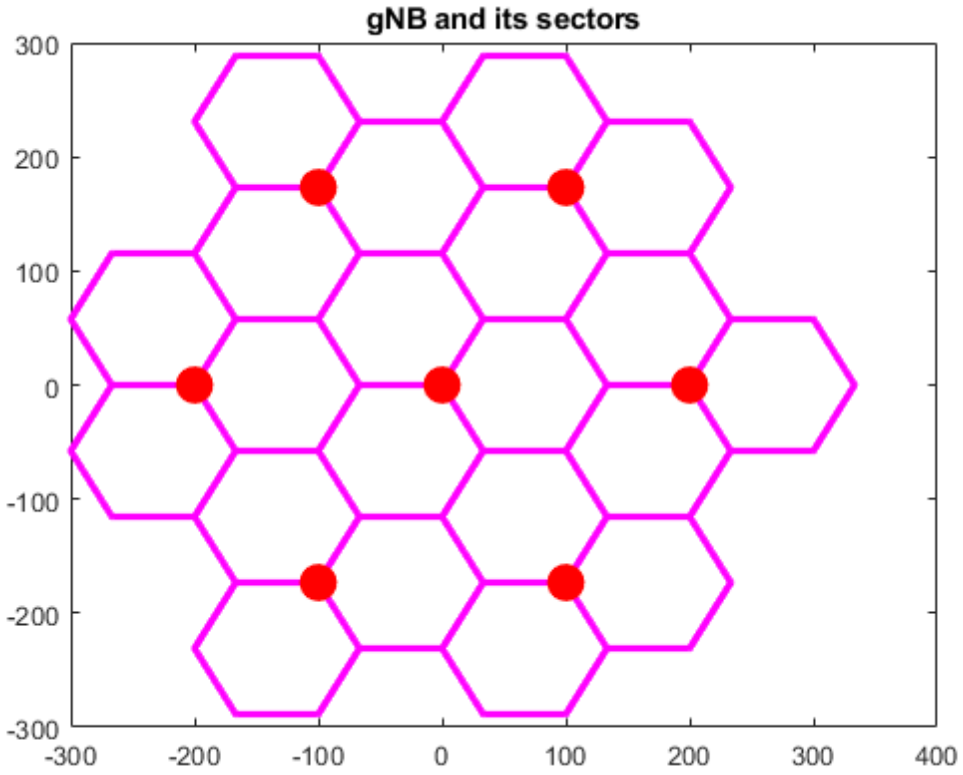

Figure 16: Hexagon grid with 7 gnBs dense Urban case

4.1.1 SINR for Rural Profile

1. Each antenna radiation pattern of Base station is shown in Figure 1.
2. Each Base station has 3 such antenna. They have bearing angles 0,120,240.
3. Frequency of carrier = 700 MHz.
4. Antenna height = 35m
5. UT height = 1.5m.
6. Bandwidth = 20MHz.
7. Intersite distance = 1732m.
8. UE noise figure = 7dB.
9. Antenna max gain = 8dBi.
10. Power transmitted = 49dBm
11. Figure 17 is SINR(dB) for Rural LOS case and Figure 18 is SINR (dB) for Rural NLOS case
12. As we can see in Figure 17 (LOS case)large area falls under high SINR than Figure 18 (NLOS case)

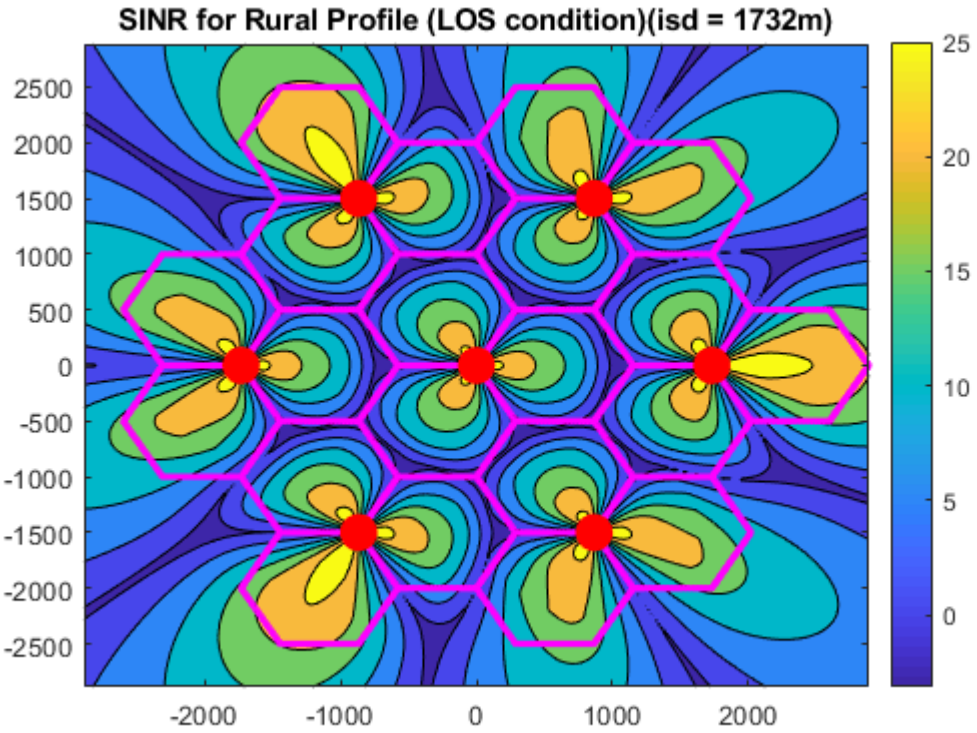

Figure 17: SINR(dB) for Rural LOS case

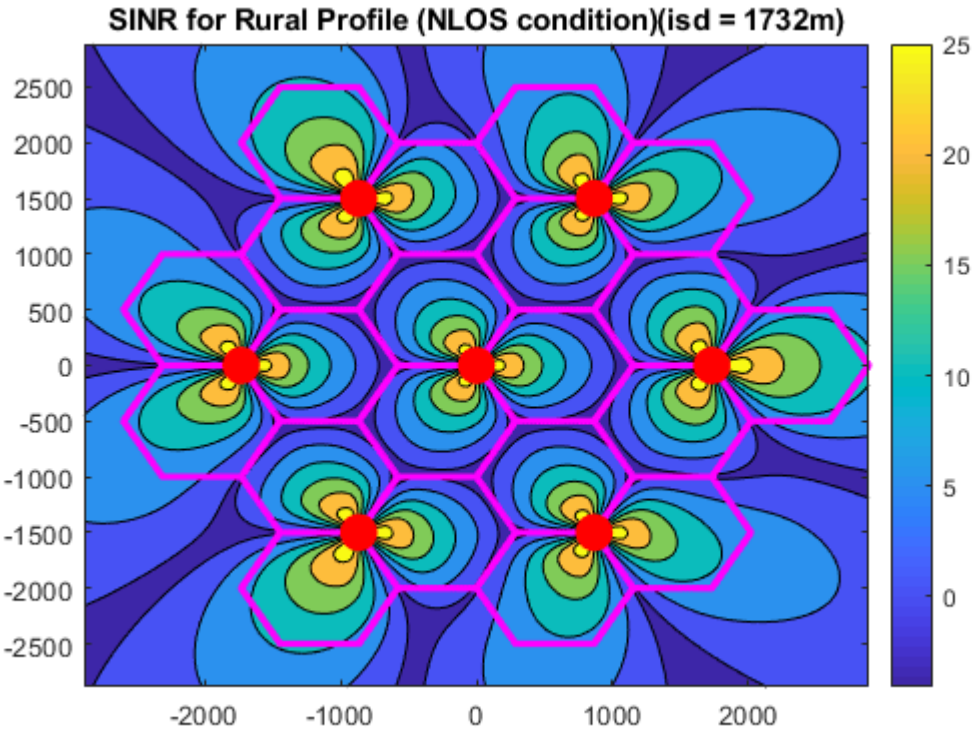

Figure 18: SINR(dB) for Rural NLOS case

4.1.2 SINR for dense Urban Profile

1. Each antenna radiation pattern of Base station is shown in Figure 1.
2. Each Base station has 3 such antenna. They have bearing angles 0,120,240.
3. Frequency of carrier = 4 GHz.
4. Antenna height = 25m
5. UT height = 1.5m.
6. Bandwidth = 20MHz.
7. Intersite distance = 200m.
8. UE noise figure = 7dB.
9. Antenna max gain = 8dBi.
10. Power transmitted = 44dBm
11. Figure 17 Figure 19 is SINR(dB) for Urban LOS case and Figure 20 is SINR (dB) for Urban NLOS case
12. In this case the NLOS case (Figure 20) has high SINR coverage than LOS case (Figure 19). Because intersite distance is low, the interference in Urban case is stronger. So NLOS case has higher SINR coverage.

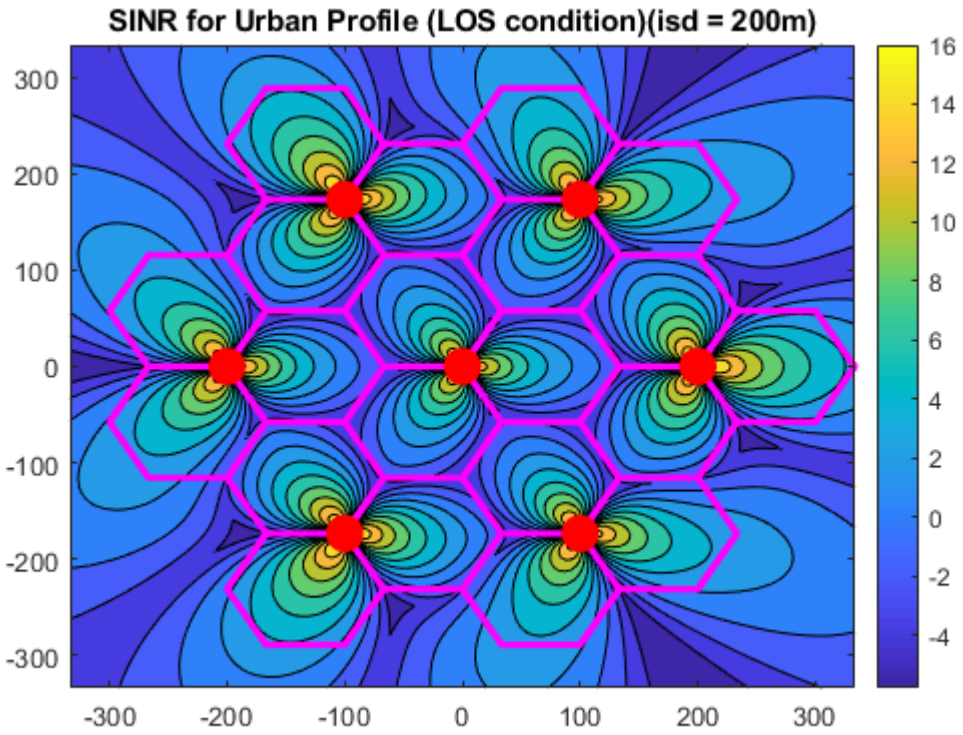

Figure 19: SINR(dB) for Urban LOS case

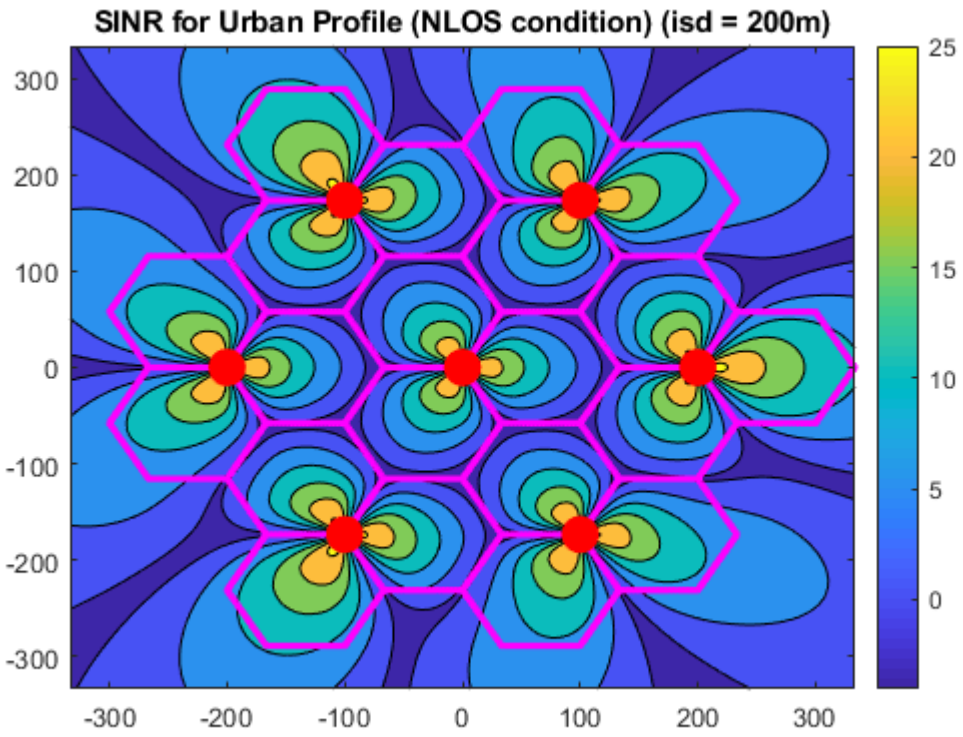

Figure 20: SINR (dB) for Urban NLOS case

4.2. Channel response

For the channel response we sent OFDM pilots through channel. As we know using OFDM ISI will be eliminated and output signal can be written as $Y = HX$, where H is diagonal matrix. Each element in the H is channel response at that particular frequency sub carrier.

Channel response is plotted for single link (BS to UE) with following parameters.

1. Frequency of sub carrier = 4GHz
2. Bandwidth = 122.88MHz
3. BS antenna element max gain = 8dBi
4. UE antenna element max gain = 5dBi

4.2.1 Channel response for InH_A(Indoor hotspot)

1. BS Antenna height: 3m
2. UE location: [5,5,1.5]m.
3. UE speed: 3Km/h.

Channel response is plotted in Figure 21.

4.2.2 Channel response for UMa_A(urban macro)

1. BS Antenna height: 25m
2. UE location: [10,10,1.5]m.
3. UE speed: 30Km/h.

Channel response is plotted in Figure 22

4.2.3 Channel response for UMi_A(urban micro)

1. BS Antenna height: 25m
2. UE location: [10,10,1.5]m.
3. UE speed: 30Km/h.

Channel response is plotted in Figure 23

4.2.4 Channel response for RMa_A(Rural macro)

1. BS Antenna height: 35m
2. UE location: [50,30,1.5]m.
3. UE speed: 30Km/h.

Channel response is plotted in Figure 24.

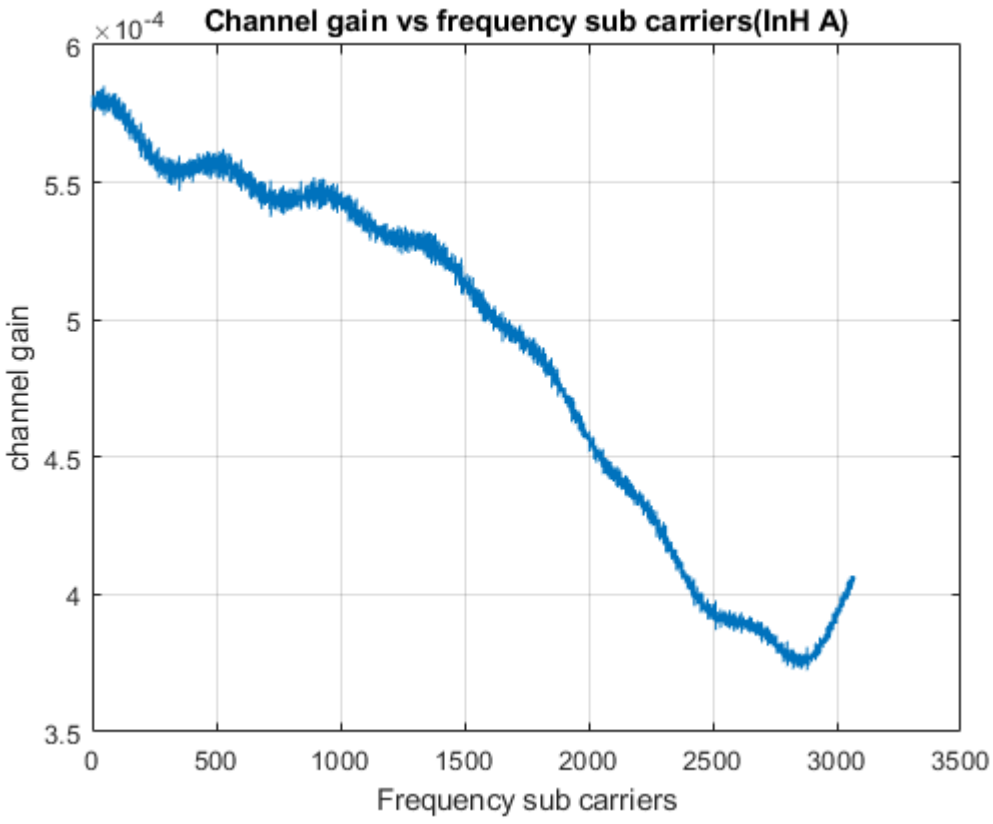

Figure 21: Channel response for Indoor Hotspot profile

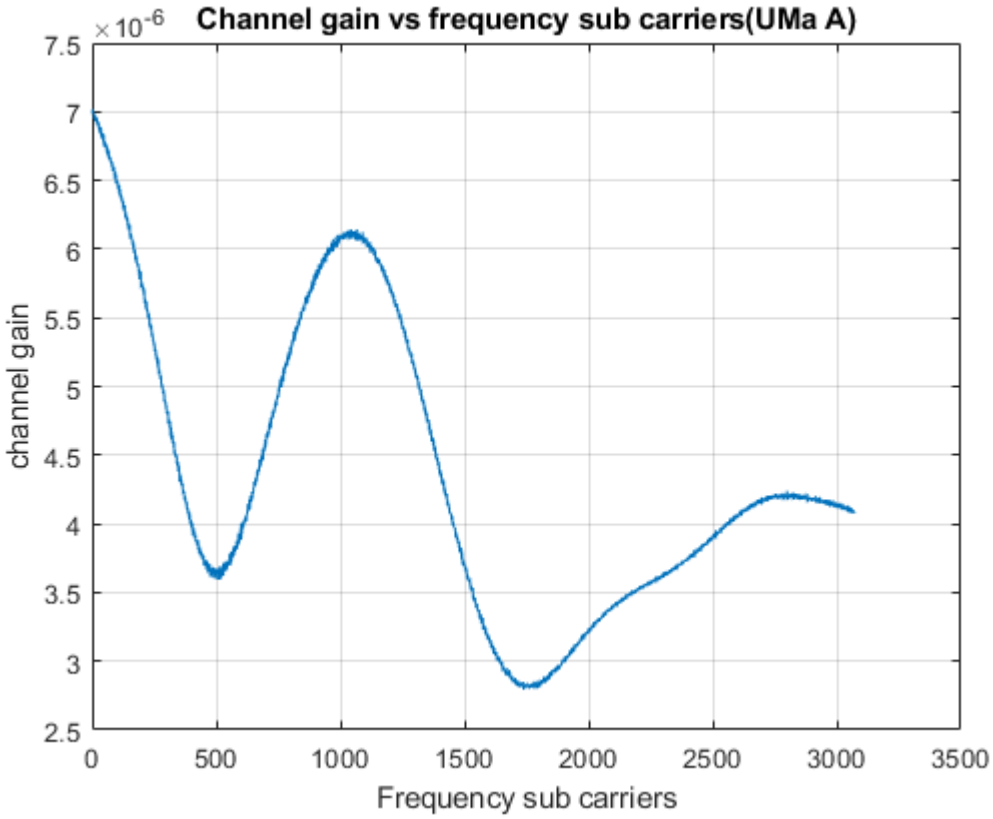

Figure 22: Channel response for Urban macro profile

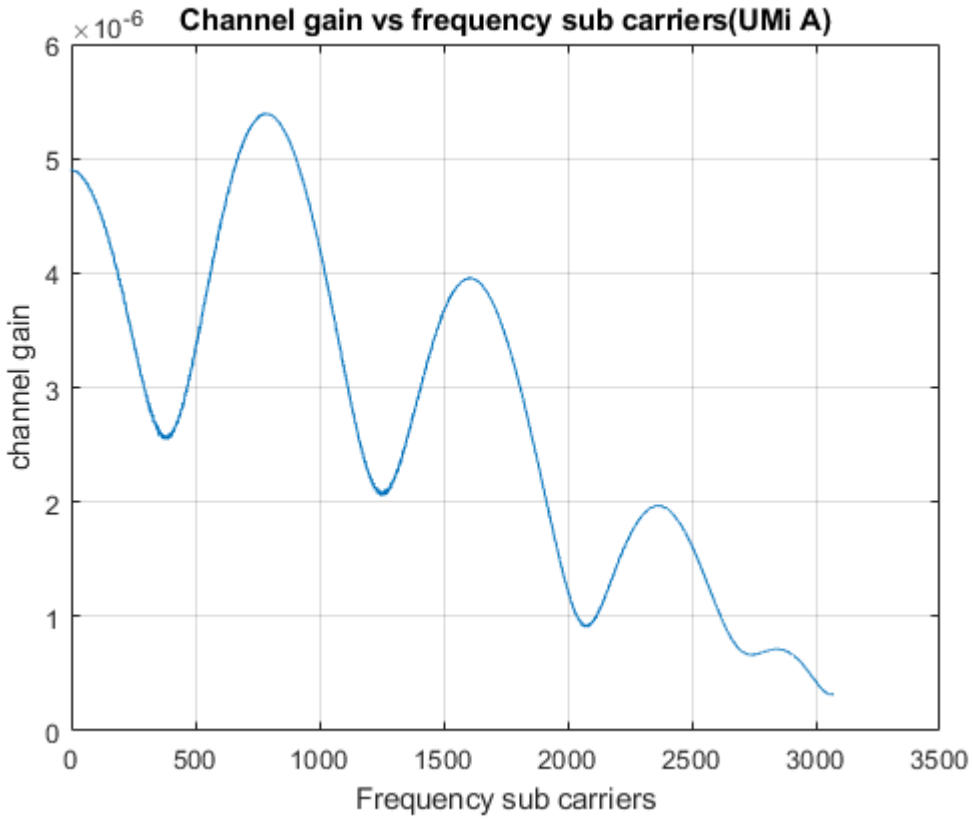

Figure 23: Channel response for Urban micro profile

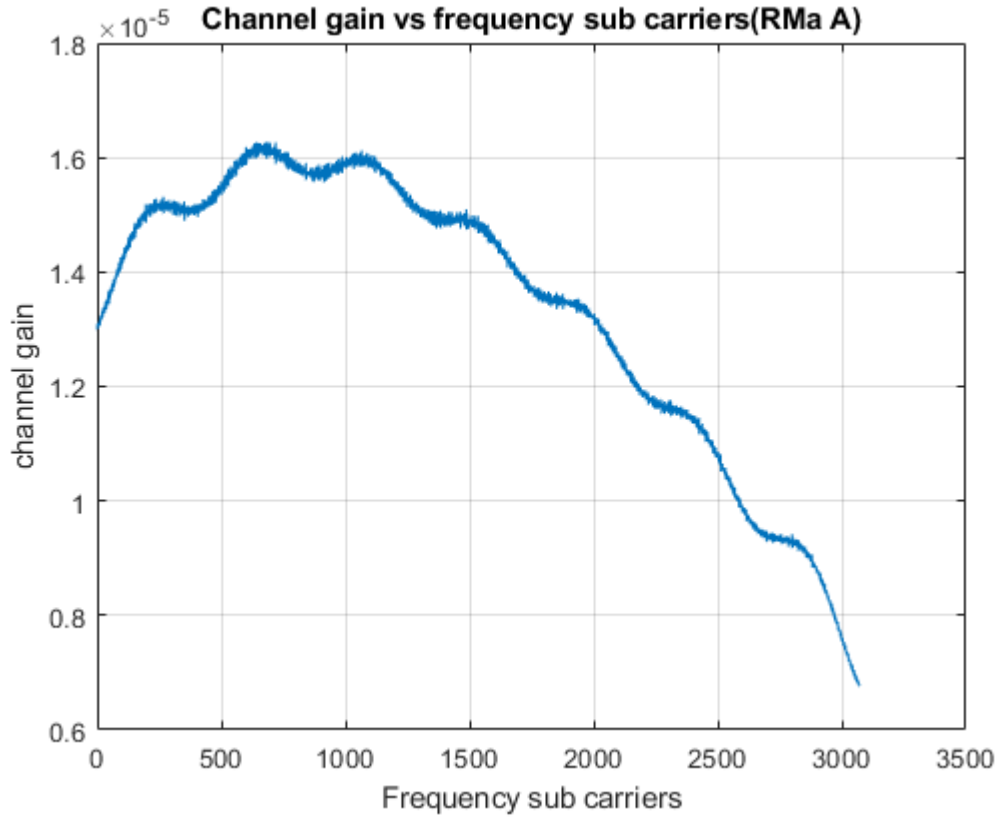

Figure 24: Channel response for Rural Macro profile

Chapter 5

Summary

The main advantage of the 3GPP geometry based stochastic channel modelling is that the scatterers are defined based on the angles of departure and angles of arrival, i.e. terminal perspective, rather than defining the physical position of the scatterers in the simulation area like a few other channel models. If physical positions are used, it is difficult to extract parameters using measurements contrary to the case of the GSCM

channel model. Hence GSCM is currently more widespread and is the preferred candidate for 5G channel modelling in standardization efforts.

The channel code written is not fully spatially consistent, that is it fails to capture scenarios where the users are in close proximity, as the channels are generated independently for each user, regardless of the distance between users. This can be improved by incorporating the spatial consistency procedure as mentioned in Chapter 5 in [3].

5.1. Potential extensions and future work

The Matlab code written is for the case of a single user in a sector. The code has to be extended to be able to support the simulation of multiple gNBs and UEs per sector. Once the codes for a single UE and a single channel link is verified, this extension needs to done and has to be verified in a similar manner, before using them for simulating the test environments for evaluation procedures.

Also the channel model can be further improved for simulating certain test scenarios by incorporating advanced modelling components like Oxygen absorption, random cluster number, ground reflection, UT rotation, blockage, spatial consistency and modelling of propagation delay and intra cluster angular and delay spreads for incorporating large antenna size and large number of antenna elements.

The modelling procedure for the above mentioned advanced components along with the corresponding step in the channel generation procedure , in which it is to be incorporated and the recommended conditions in which they can be done in addition to the normal channel generation procedure are described in the ITU document M.2412.

References

[1] **Report ITU-R M.2410-0**
Minimum requirements related to technical performance for IMT-2020 radio interface(s)

[2] **Report ITU-R M.2411-0**
Requirements, evaluation criteria and submission templates for the development of IMT-2020

[3] **Report ITU-R M.2412-0**
Guidelines for evaluation of radio interface technologies for IMT-2020

[4] **IST-WINNER II Deliverable 1.1.2 v.1.2.,** "WINNER II channel models, IST-WINNER2, Tech. Rep., 2008.

[5] **3GPP TR 38.901 version 14.3.0 Release 14),** Study on channel model for frequencies from 0.5 to 100 GHz